PETROGRAPHY AND MINERAL CHEMISTRY OF NORTHEAST AFRICA (NEA) 053. X. Shehaj[1,2,3], E. Ammannito[2], G. Pratesi[3]. (xhonatan.shehaj@unitn.it) [1]Dipartimento di Fisica, Università degli Studi di Trento, Via Sommarive 14, 38123 Trento, Italy; [2]Agenzia Spaziale Italiana, Via del Politecnico, 00133 Roma, Italy; [3]Dipartimento di Scienze della Terra, Università degli Studi di Firenze, Via G. La Pira 4, 50121 Firenze, Italy.

Introduction: Martian meteorites, the only direct samples currently available from Mars, provide a unique opportunity to investigate Martian igneous processes [e.g., 1]. These meteorites are traditionally classified into three main lithological groups: shergottites, nakhlites, and chassignites, which are mantle-derived mafic to ultramafic rocks that crystallized as extrusive lavas or in shallow intrusive (hypoabyssal) settings within the Martian crust [1]. Shergottites, which are predominantly basalts (*sensu lato*), reveal important information about volcanic and magmatic activity on Mars [1-4]. Petrographic and mineral-chemistry features preserved in these meteorites record key magmatic processes [5-9], including magma dynamics [10]. Here, we report the petrographic and mineral chemistry study of Northeast Africa (NEA) 053, a unique Martian meteorite preserving fine- and coarse-grained domains within a single sample.

Materials and Methods: A fragment of NEA 053 (~250 mm²) was embedded in epoxy resin and prepared as a polished thick section for detailed electron microscope analyses. Electron microscope measurements were conducted using a Zeiss EVO MA15 scanning electron microscope (SEM), equipped with a 40 mm^2 Silicon Drift Detector (SDD) and Oxford Ultim Max system. Semiquantitative Energy Dispersive X-ray Spectroscopy (EDS) point analyses were performed at 15 kV accelerating voltage and 700 pA nominal beam current. Quantitative compositional point analyses were carried out using a JEOL JXA/8230 Electron Microprobe Analysis (EMPA). Analyses of olivine and pyroxene were performed at an accelerating voltage of 15 kV and a beam current of 20 nA, using a beam with a 3 µm spot size. For maskelynite, a defocused beam with a 10 µm spot size was employed under the same voltage and current conditions.

Results: Northeast Africa 053 has a porphyritic texture, primarily characterized by pyroxene and olivine megacrysts (up to ~ 2.2 mm) set in a groundmass composed of lath-like maskelynite (shocked plagioclase) and pyroxene grains (~ 100 µm in length). In the investigated section, pyroxene crystals display a distinct grain-size layering, mainly characterized by an irregular-shaped, fine-grained layer (2-4 mm in thick) interposed in a coarse-grained domain (Figure 1). On this basis, we define two main textural domains: a fine-grained layer with pyroxene crystals typically 200-300 µm in size, and a coarse-grained domain, characterized by pyroxene megacrysts, typically ranging from 500 µm up to 2.2 mm, as illustrated in Figure 1. In contrast, olivine megacrysts are uniformly distributed. Accessory phases are evenly distributed, comprising approximately 2 vol.% of the sample. These include phosphates, Fe-Ti-Cr oxides, ilmenite, and Fe-sulfide. Melt inclusions are commonly observed within the euhedral olivine crystals. Additionally, shock-induced melt pockets and melt veins are commonly observed, comprising approximately 1.7 vol.% of the sample.

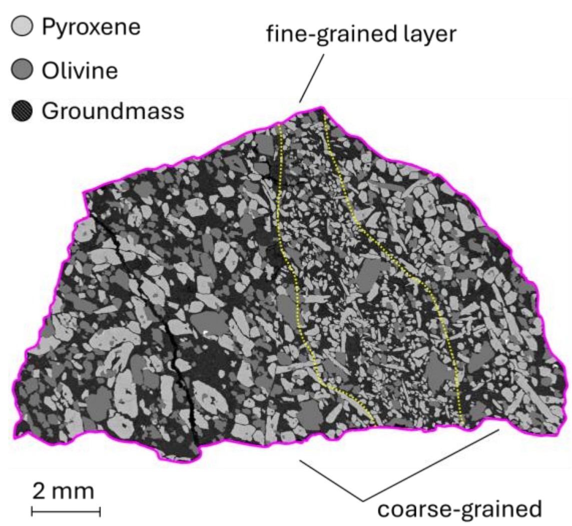

Figure 1. Phase map of the analysed portion of NEA 053, showing the distinct fine-grained layered interposed within the coarse-grained domain.

Modal mineral abundances, calculated excluding the shock-metamorphosed portion, show comparable mineral proportions across both textural domains. In the fine-grained layer, the modal mineralogy is pyroxene 55 vol.%, maskelynite 26 vol.%, olivine 17 vol.%, other minerals 2 vol%, while in the coarse-grained domain is pyroxene 53 vol.%, maskelynite 24 vol.%, olivine 21 vol.%, other minerals 2 vol%.

Pyroxene grains in both textural domains exhibit a consistent zoning pattern, typically characterized by Mg-rich pigeonite cores ($En_{68-67}Fs_{26-25}Wo_{5-7}$), augite mantles ($En_{48-46}Fs_{26-24}Wo_{26-30}$), and in some grains a defined Fe-rich pigeonite rims ($En_{39-41}Fs_{47-44}Wo_{14-15}$).

High-precision electron microprobe analyses show that the core and mantle compositions of pyroxene crystals are indistinguishable between the coarse- and fine-grained domains. In contrast, rim compositions, as well as groundmass pyroxene grains in the fine-grained layer, exhibit progressively higher FeO contents compared to their counterparts in the coarse-grained domain (Figure 2).

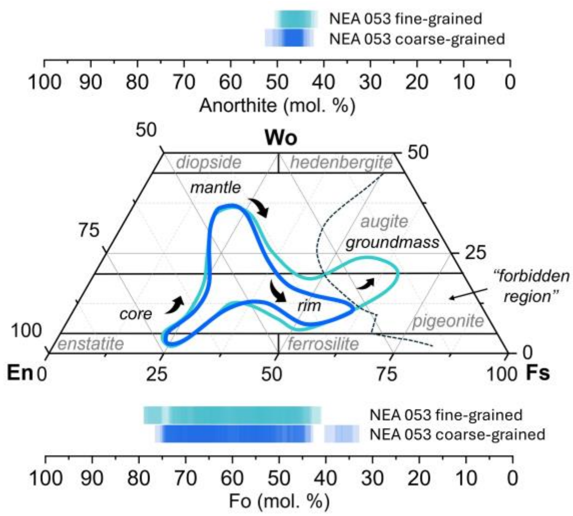

Figure 2. Comparison of pyroxene, olivine, and maskelynite compositions between fine- and coarse-grained domains in NEA 053. The dash line field in the pyroxene quadrilateral diagram represents the pyroxene "forbidden region" [11].

No significant compositional differences are observed, with analytical uncertainty, for olivine and maskelynite between fine- and coarse-grained domains (Figure 2). Olivine megacryst exhibit well-defined core-to-rim zoning, with $Fo_{72\pm3}$ in the cores and $Fo_{62\pm6}$ at the rim. Maskelynite display a homogeneous composition (An_{51-43}) and consistent grain size across both coarse- and fine-grained domains.

Discussion and Conclusion: Pyroxenes from both fine- and coarse-grained domains share similar core-to-rim chemical evolution, supporting crystallization from a single magma body. The textural contrast, however, is pronounced, as differences in grain size imply contrasting cooling paths. Coarse-grained domain likely experienced slower early cooling compared to the fine-grained layer. These observations are best explained by crystallization in spatially distinct thermal regimes within the same magmatic system. Additionally, late-stage pyroxene (rims and groundmass) in the fine-grained layer shows higher FeO contents, further supporting a higher cooling rate than in the coarse-grained domain (Figure 2). We propose that the two textural domains in NEA 053 originally formed in distinct zones within a single, evolving crystal mush system.

Acknowledgments: This research was financed by the Space It Up project funded by the Italian Space Agency, ASI, and the Ministry of University and Research, MUR, under contract n. 2024-5-E.0 – CUP n. I53D24000060005. The research activity of X. Shehaj has been conducted during the Italian national inter-university PhD program in Space Science and Technology.

References: [1] Udry A. et al. (2022) *JGR Planets, 125*, e2020JE00652; [2] Goodrich C. A. et al. (2003) *GCA,* 67: 3735–3772; [3] Van Niekerk D et al. (2007) *MAPS,* 42: 1751-1762; [4] Usui T. et al. (2008) *GCA,* 72: 1711-1730; [5] Sarbadhikari, A. B. et al. (2009) *GCA,* 73: 2190-2214; [6] Peslier, A. H. et al. (2010) *GCA,* 74: 4543-4576; [7] Mari N. et al. (2020) *MAPS,* 55: 1057-1072 ; [8] Benaroya S. et al. (2024) *GCA,* 370: 41-65. [9] Shehaj X. et al. (2025) *JGR Planets,* 130: e2024JE008885; [10] Ostwald A. et al. (2024) *GCA*, 380: 1-17; [11] Lindsley D. H. (1983) *Am. Min*. 68:477–493.